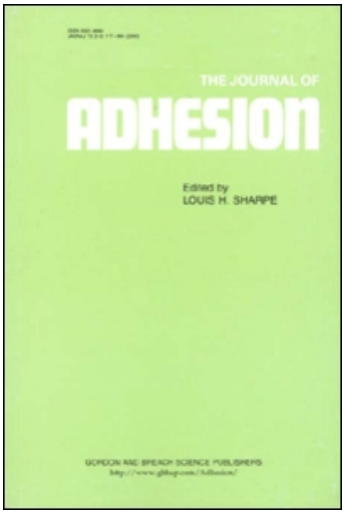

The Journal of Adhesion
Publication details, including instructions for authors and subscription information:
http://www.informaworld.com/smpp/title~content=t713453635

Finite Element Analysis if Interfacial Friction and Slip in Composites with Fully Unbonded Filler

E. Ghassemieh[a]
[a] School of Mechanical and Manufacturing Engineering, Loughborough University, Loughborough, United Kingdom

Online publication date: 08 September 2010

To cite this Article Ghassemieh, E.(2002) 'Finite Element Analysis if Interfacial Friction and Slip in Composites with Fully Unbonded Filler', The Journal of Adhesion, 78: 4, 271 — 295
To link to this Article: DOI: 10.1080/00218460210936
URL: http://dx.doi.org/10.1080/00218460210936

The Journal of Adhesion, 78: 271–295, 2002

0021-8464/02 $12.00 +.00

FINITE ELEMENT ANALYSIS OF INTERFACIAL FRICTION AND SLIP IN COMPOSITES WITH FULLY UNBONDED FILLER

E. Ghassemieh
School of Mechanical and Manufacturing Engineering,
Loughborough University, Loughborough, United Kingdom

A finite element model is developed to predict the stress-strain behaviour of particulate composites with fully unbonded filler particles. This condition can occur because of the lack of adhesion property of the filler surface. Whilst part of the filler particle is separated from the matrix, another section of filler keeps in contact with the matrix because of the lateral compressive displacement of the matrix. The slip boundary condition is imposed on the section of the interface that remains closed. The states of stress and displacement fields are obtained. The location of any further deformation through crazing or shear band formation is identified. A completely unbonded inclusion with partial slip at a section of the interface reduces the concentration of the stress at the interface significantly. Whereas this might lead to slightly higher strength, it decreases the load transfer efficiency and stiffness of this type of composite.

Keywords: Particulates composites; Finite element analysis; Stress-strain behaviour; Stiffness; Strength; Particulate filler; Matrix-filler interface; Failure

INTRODUCTION

Adhesion between the two phases is often a critical factor in determining the ultimate strength of a composite material. The level of bonding of inclusions to the matrix is also one of the dictating aspects in load transfer.

The level of bonding of the matrix and filler phases depends on the surface condition of the filler. The viscosity of the resin at the time of application and the amount of the wetting of the filler are other factors

Received 11 June 2001; in final form 30 August 2001.
Address correspondence to E. Ghassemieh, School of Mechanical and Manufacturing Engineering, Loughborough University, Loughborough, LE11 3TU, UK. E-mail: E.Ghassemieh@lboro.ac.uk

in quality of the bonding of the components of the composite. Stiffer filler than resin and similar thermal expansion coefficient for the components can assist the filler-matrix bonding.

If any of these required conditions for perfect bonding are not fulfilled the adhesion between the matrix and filler would not be achieved. Treating the particles with a coating can affect and control the adhesion between the matrix and filler. For example, hexamethyldisilazane and commercial silane coupling agents reduce the adhesion between filler and matrix [1].

In this paper the stress field in a composite with fully unbonded rigid particles is analysed and the effect of poor adhesion on the ultimate strength and stiffness of the composite is studied.

Most of the theories which explain the reinforcing action of a filler assume perfect adhesion between the filler and the polymer matrix. The case of imperfect adhesion was, however, discussed theoretically by Sato and Furukawa [2]. They assumed that the nonbonded particles act as holes and, therefore, predicted a decrease in modulus with increasing filler content. One can argue that the nonbonded particles do not act entirely as holes since they also restrain the matrix from collapsing. A change of the matrix-filler adhesion has a smaller effect on modulus than on strength. The latter is much more dependent on surface pretreatment. In fact, the degree of adhesion does not appear to be an important factor as long as the frictional forces between the phases are not exceeded by the applied stress. In most filled systems there is a mismatch in the coefficients of thermal expansion which is reflected as a mechanical bond resulting from thermally induced stresses. Brassell [3] found that the degree of bonding between the phases does not appear to have any influence on mechanical properties at liquid nitrogen temperature and this was attributed to the compressive stresses on the filler particle. In most cases, even if the adhesion between phases is poor, the theories remain valid as long as there is not any relative motion across the filler-matrix interface (no slip case) [4].

However, as soon as the frictional forces are exceeded and the relative motion of filler and matrix is possible the stresses around the interface are affected significantly. In this paper we study the condition that there is no bonding between the filler and matrix. The two phases are free in movement unless they come into physical contact as a result of displacement.

The stress-strain at this part depends on the friction between the filler and matrix at the contacting face. This state is simulated by allowing a slip condition at this part of the interface. The slip coefficient indicates the level of friction.

DEVELOPMENT OF THE PREDICTIVE MODEL

Working Equations of the Model

We start with the governing equations of creeping (Stokes) flow of incompressible fluids which include the momentum and continuity equations. By applying a penalty method, using an appropriate penalty equation, the terms for pressure are eliminated. The resultant equations will be identical to elasticity equations. This has given us the advantage of using the same code for the simulation of the behaviour of the composite materials in both solid and fluid states. A Galerkin weighted residual method is used to obtain the finite element formulation of the working equations. Detail of the working equations are already published elsewhere [5] (Appendix).

Computational Domain Geometry and Boundary Conditions

In the finite element approximation of axisymmetric solids, the continuous structure or medium is replaced by a system of axisymmetric elements interconnected at nodal points. It is assumed that the composites filled with particles (assumed to possess symmetry) could be approximated by a unit cell shown in Figure 1a. When this unit cell is rotated 360° around axis OD, a hemisphere embedded in a cylinder is produced [6].

The boundary conditions imposed for analysing the tensile load applied on a particulate filled composite are as follows [7]:

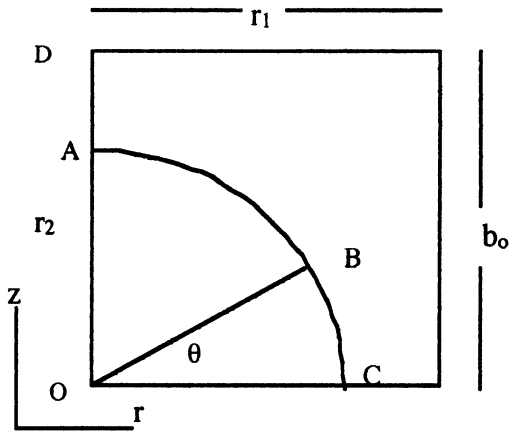

FIGURE 1a Axisymmetric unit cell.

$$v_z = 0 \quad \text{on } Z = 0 \tag{1a}$$

$$v_z = V \quad \text{on } Z = b_0 \tag{1b}$$

Here V is a prescribed constant while U is determined from the condition of vanishing of the average lateral traction rate, *i.e.*:

$$\sigma_{rr} = 0 \quad \text{on } \mathrm{r} = \mathrm{R}_0 \tag{2}$$

which means that every point along $r = R_0$ is stress free. Under these conditions the outer sidewall of the cell does not remain straight and vertical. However, for the entire specimen under tension the stress component σ_{rr} on the outer boundary is zero. The chosen unconstraint boundary condition is proved to simulate more accurately the properties of this type of composite. Detail of the comparison of the boundary conditions in modelling of the properties of particulate composites is already reported [5]. On the part AB of the interface the filler and matrix are separated. On the part BC of the interface the filler particle and the matrix are in contact. A slip boundary condition is applied on this part of the interface. A more detailed explanation of the state of the interface is presented in the further sections of this paper.

The finite element mesh used in the analysis is shown in Figure 1b. The elements are nine-noded biquadratic. The mesh is refined at the interface region.

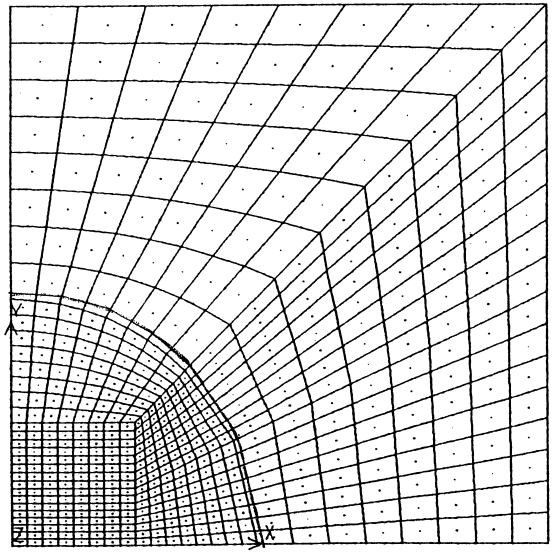

FIGURE 1b Mesh.

Slip Boundary Condition for Fully Debonded Particle

When there is no slip at the interface of the matrix and filler, the relative displacement of the two phases is zero, whereas in the case of slip the relative displacement of the two phase is not zero and the boundary condition is described by Naviers slip relation, which is a third kind (Robin or convective) of boundary condition:

$$(\boldsymbol{\beta\tau} \cdot \mathbf{n} + \mathbf{v}) \cdot \mathbf{t} = \mathbf{0} \tag{3}$$

Complementary with the above boundary condition is the following relation which ensures there is no relative radial displacement of the two phases.

$$\mathbf{v} \cdot \mathbf{n} = \mathbf{0} \tag{4}$$

Where:

$\boldsymbol{\beta}$ = slip coefficient
$\boldsymbol{\tau}$ = stress tensor
$\mathbf{n}$ = unit vector normal to the interface
$\mathbf{t}$ = unit vector tangential to the interface
$\mathbf{v}$ = relative displacement of the two phases

From the slip boundary equations and the usual stress and displacement relations the components of the slip displacements are obtained as follows [8]:

$$v_1 = -\mu\beta n_2 \left[2\left(\frac{\partial v_1}{\partial x_1} - \frac{\partial v_2}{\partial x_2} \right) n_1 n_2 + \left(\frac{\partial v_1}{\partial x_2} + \frac{\partial v_2}{\partial x_1} \right) \left(n_2^2 - n_1^2 \right) \right] \tag{5}$$

$$v_2 = \mu\beta n_1 \left[2\left(\frac{\partial v_1}{\partial x_1} - \frac{\partial v_2}{\partial x_2} \right) n_1 n_2 + \left(\frac{\partial v_1}{\partial x_2} + \frac{\partial v_2}{\partial x_1} \right) \left(n_2^2 - n_1^2 \right) \right] \tag{6}$$

v_1 and v_2 are the components of displacement in the tangential and normal direction to the interface. n_1 and n_2 are the unit vector components in the tangential and normal direction to the interface. μ and β are shear modulus and slip coefficient, respectively.

We discretise the domain and write the weak formulation of the slip displacement relations. The interpolation points are chosen inside the elements adjacent to the slip boundary. The resulting stiffness matrices are assembled with other elemental matrices obtained from the working equations to form the global stiffness matrix representing the entire domain.

The matrix representation of these equations for an element located at the slip boundary results in the following equation:

$$\begin{bmatrix} a_{11}^{ij} & a_{12}^{ij} \\ a_{21}^{ij} & a_{22}^{ij} \end{bmatrix} \begin{bmatrix} v_{1j} \\ v_{2j} \end{bmatrix} = \begin{bmatrix} 0 \\ 0 \end{bmatrix} \tag{7}$$

The members of the above stiffness matrix are given as:

$$\begin{aligned} a_{11}^{ij} &= \int_{\Omega} N_i N_j d\Omega + 2n_1 n_2^2 \int_{\Omega} \mu\beta N_i N_{j,1} d\Omega \\ &\quad + (n_2^2 - n_1^2) \int_{\Omega} \mu\beta N_i N_{j,2} d\Omega \\ a_{12}^{ij} &= -2n_1 n_2^2 \int_{\Omega} \mu\beta N_i N_{j,2} d\Omega \\ &\quad + (n_2^2 - n_1^2) n_2 \int_{\Omega} \mu\beta N_i N_{j,1} d\Omega \\ a_{21}^{ij} &= -2n_2 n_1^2 \int_{\Omega} \mu\beta N_i N_{j,1} d\Omega \\ &\quad - (n_2^2 - n_1^2) n_1 \int_{\Omega} \mu\beta N_i N_{j,2} d\Omega \\ a_{22}^{ij} &= \int_{\Omega} N_i N_j d\Omega + 2n_2 n_1^2 \int_{\Omega} \mu\beta N_i N_{j,2} d\Omega \\ &\quad - (n_2^2 - n_1^2) \int_{\Omega} \mu\beta N_i N_{j,1} d\Omega \end{aligned} \tag{8}$$

N_i and N_j are the weight and shape functions, respectively.

ANALYSIS OF RESULTS

Analysis of the Contact at the Interface of an Unbonded Filler

In order to investigate the stress transfer at the interface of a debonded filler particle and matrix, we primarily study the state of displacement of the matrix in the vicinity of a void under tensile loading. For an unbonded filler in the matrix, as long as the components are not brought into contact by a lateral displacement (lateral

TABLE 1 Material Properties for the Matrix-Filler

	Input properties	
Phase	E (Gpa)	Poisson's ratio, v
Matrix	3.01	0.35
Glass Sphere	76.0	0.21

displacement and compressive stress are a result of the Poisson's contraction in tensile loading), the state of the stress and displacement in the matrix will be similar to a voided composite. So the displacement of the matrix at the boundary of the void is used to find the contact and separation point of the unbonded particle.

An epoxy resin filled with glass beads is chosen as the matrix and the filler, respectively. The input properties of the phases are reported in Table 1.

The radial displacement at the boundary of a void in a polymer matrix is estimated by our model. The results are presented in Figure 2

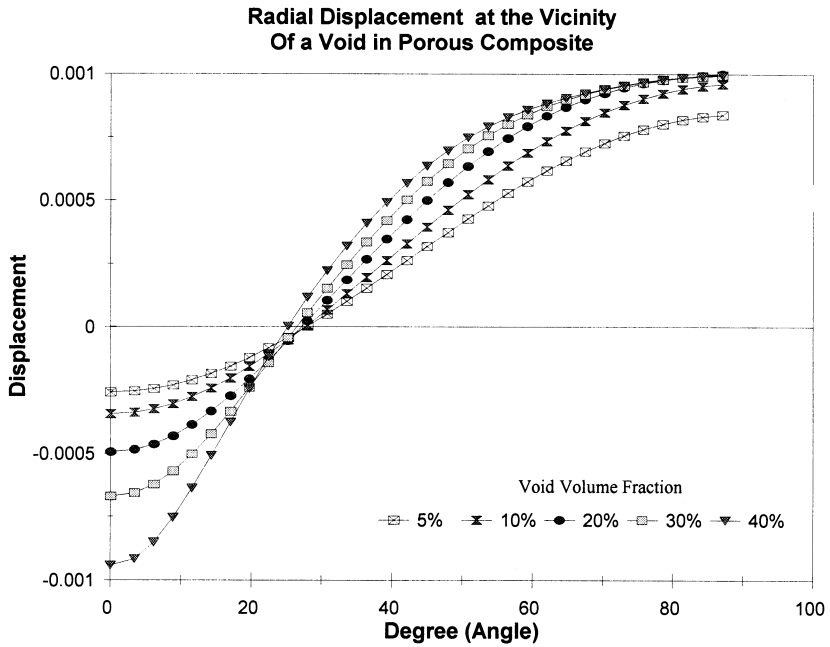

FIGURE 2 Displacement of the matrix at the boundary of a void in a porous composite.

for different volume fractions. The displacement at the pole of the void is positive for all volume fractions. Displacement is negative at the equator up to an angle of about 23 degrees.

Therefore, it is expected, for a composite with an unbonded filler particle, that the filler and matrix are in contact at the region of the equator up to about 23 degrees (BC in Figure 1a). They are separated from this point to the pole of the filler particle (AB in Figure 1a). The level of the stress transfer at the contacting interface depends on the friction between the two phases.

If the frictional force acting on the interface is high enough it can prevent the particle and matrix from having relative tangential movement. This case is studied elsewhere [9]. If the frictional force is weak, the tangential displacement occurs and, hence, the slip boundary condition is imposed for this case. The slip coefficient controls the extent of relative movement of the matrix and the filler particle.

The frictional force between the two phases is proportional to the normal stress acting on the interface. Therefore, in the segment closer to the pole, it is equal to zero which shows that no stress transfer occurs. In the other segment which experiences a compressive stress, the frictional force rises. This frictional force acts in the opposite direction to the tangential stress and is proportional to the normal stress, so that:

$$F_t = \mu F_n \tag{9}$$

The value of frictional force determines whether there is any relative tangential displacement between filler and matrix or not. The friction or the freedom of movement of the two phases with respect to each other can be defined by the slip Equation (3).

In this equation, β, the slip coefficient, indicates the level of the relative movement. Therefore, the higher the friction coefficient, μ, the lower the slip coefficient, is expected to be and *vice versa*. The displacement of the matrix at the interface of a fully debonded composite is presented in Figure 3a. The displacement at the contact point with the filler is very small compared with the separated part.

The displacement of the matrix for a composite with unbonded particles remains negative on the slipping part of the interface in the presence of the filler particle for all volume fractions (Figure 3b) which is similar to the border of the void. Although at higher volume fractions of 30% it tends to very small values, close to zero, near the equator of the filler particle. This shows that the filler stays in contact with the matrix at low volume fractions.

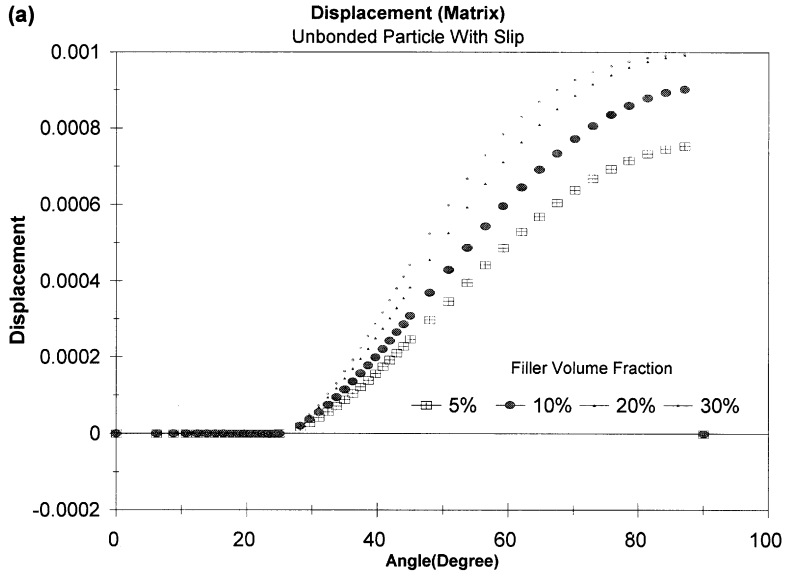

FIGURE 3a Displacement of matrix and filler at the interface of two phases in a composite with unbonded filler particle for different volume fractions.

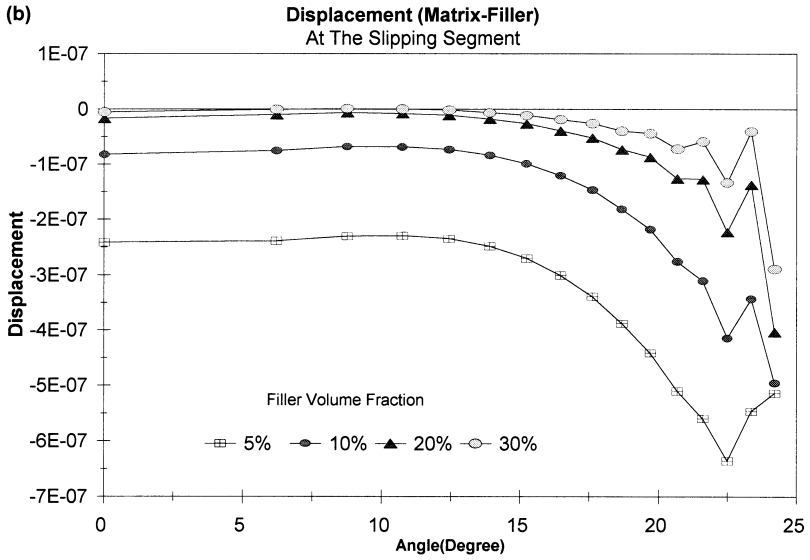

FIGURE 3b Displacement of matrix and filler at the part of the interface that matrix and filler are in contact in a composite with unbonded filler particles (different volume fractions).

The radial stresses at this part are compressive and negative for all volume fractions up to 20% (Figure 4). This confirms that the matrix and the filler are in contact at the slipping part. At higher volume fraction, though, the stresses become positive which can result in losing contact of the component at this segment of the filler particle at the equator. In a composite with partially debonded filler or an interfacial crack, any further crack propagation is stable. This case is analysed separately [9]. However, in the composite with fully unbonded filler, which is the case we now are looking at, any further physical separation or making contact between the two phases is unstable. Our result here shows that any further separation can be from the equator. However, any change in the contact points result in the new state of stick and slip on the boundary and unstable contact points and stresses. For the voided composite the radial stresses are almost zero for all the volume fractions, which indicates a free boundary.

In comparing the results of our model and experimental results for the completely debonded particle it should be noticed that in our model we ignore the thermal residual stresses. These stresses build up as a result of the mismatch of the thermal expansion

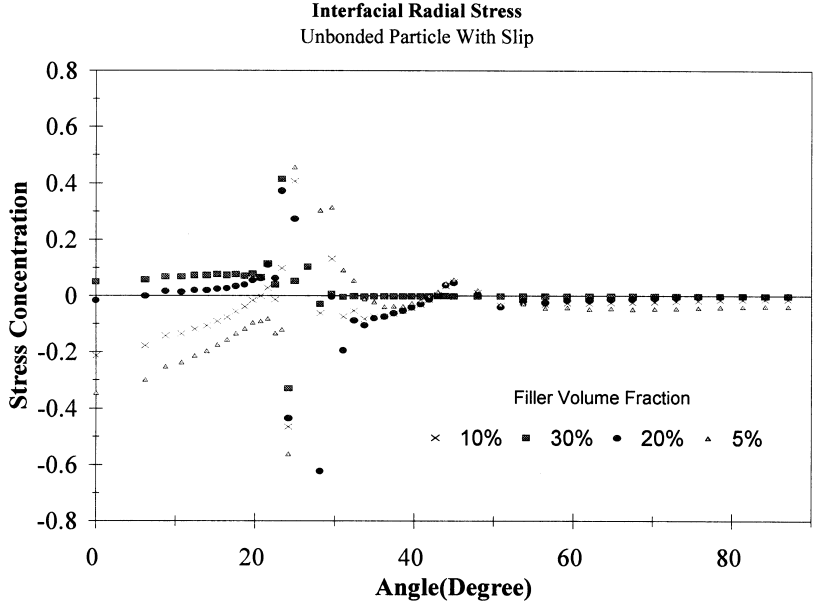

FIGURE 4 Radial stress concentration at the interface of the filler and matrix for a composite with fully unbonded filler (different volume fractions).

coefficients of the two phases. The thermal expansion coefficient of the polymer is almost ten times that of the glass. The thermal residual stresses can cause the angle of separation to be smaller than 68° from the pole.

Stress Distribution at the Interface of Unbonded Filler

The Von Mises stresses at the interface of the voided and unbonded composite are compared (Figure 5a–b). In an unbonded filler case this maximum is observed at the end of the contact point (Figure 5a). The maximum of the Von Mises stress for the voided composite occurs at the equator. For the fully bonded particle there are two locations of maxima, one at the pole and the other at about 45 degrees (Figure 5b).

The radial, tangential and Von Mises stresses at the interface are calculated for composite with 10% volume fraction of unbonded particles. All the stresses show a similar trend. However, the maximum for radial stress is lower than for the tangential and Von Mises

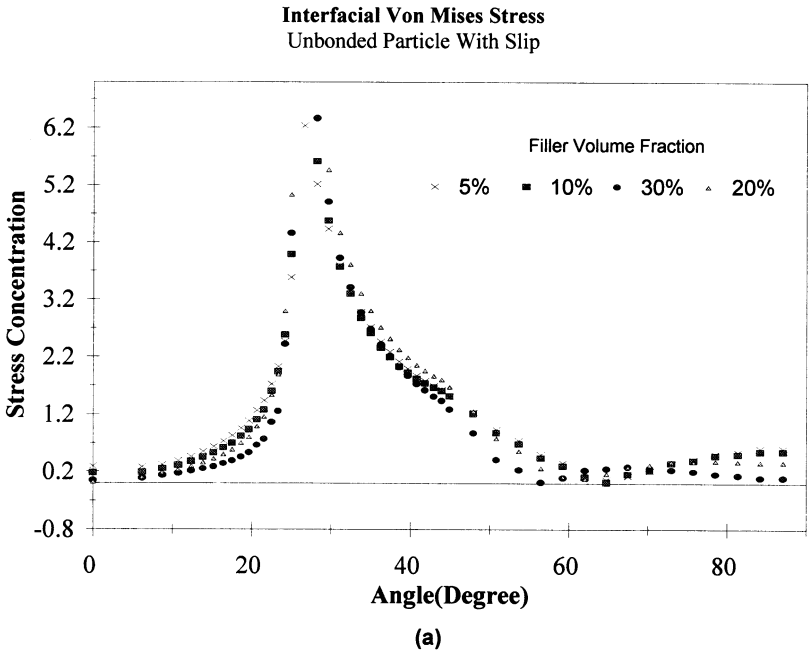

FIGURE 5a Von Mises stress concentration at the interface of the filler and matrix for a composite with fully unbonded filler (different volume fractions).

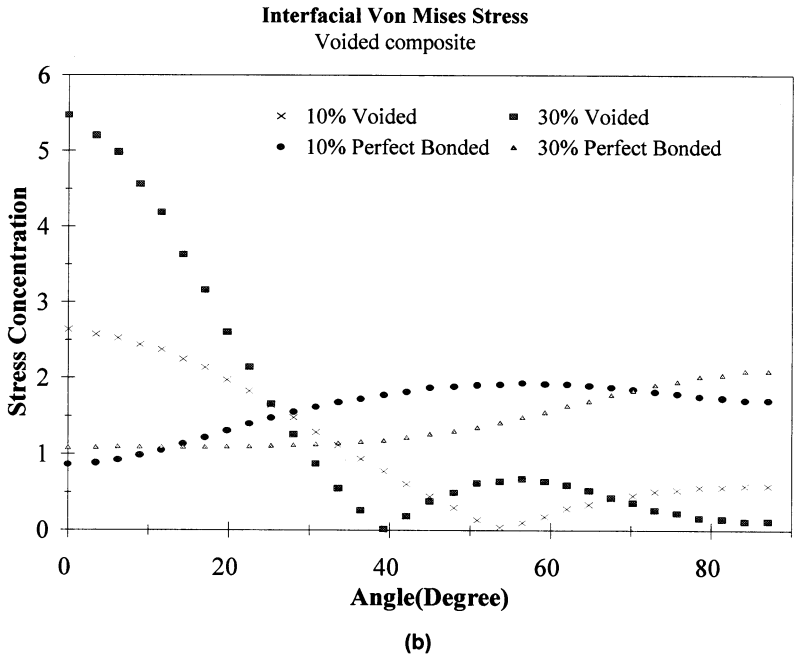

FIGURE 5b Von Mises stress concentration at the interface of the filler and matrix for a composite with perfect bonding and a composite containing voids (different volume fractions).

stresses (Figure 6a). At the border of a void in the composite under the same loading the radial stress is nearly zero, whereas the tangential and Von Mises reach much higher concentrations with the maximum at the equator (Figure 6b).

For a partially debonded particle with bonding at part of the interface, the radial stress is much smaller than the other two stresses, indicating a biaxial state of stress. The interfacial stresses observed in a composite with perfect bonding between the components are triaxial. Therefore, the composites with poorer bonding are expected to be tougher than a composite with perfectly bonded fillers. In the case of the fully debonded filler, the load transfer from the matrix to filler is reduced. At the same time, the stresses at the interface are smoother than partially bonded filler.

The radial stresses at the interface of the filler and matrix are predicted for different slip coefficients. Different slip coefficients simulate different friction forces between the contacting surfaces of the filler and matrix.

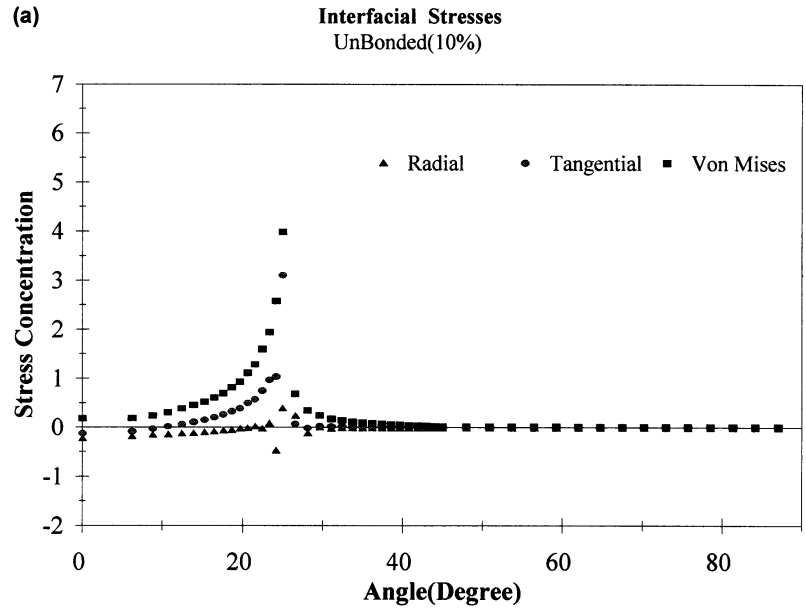

FIGURE 6a Interfacial stress concentrations for a composite with fully unbonded filler (volume fraction 10%).

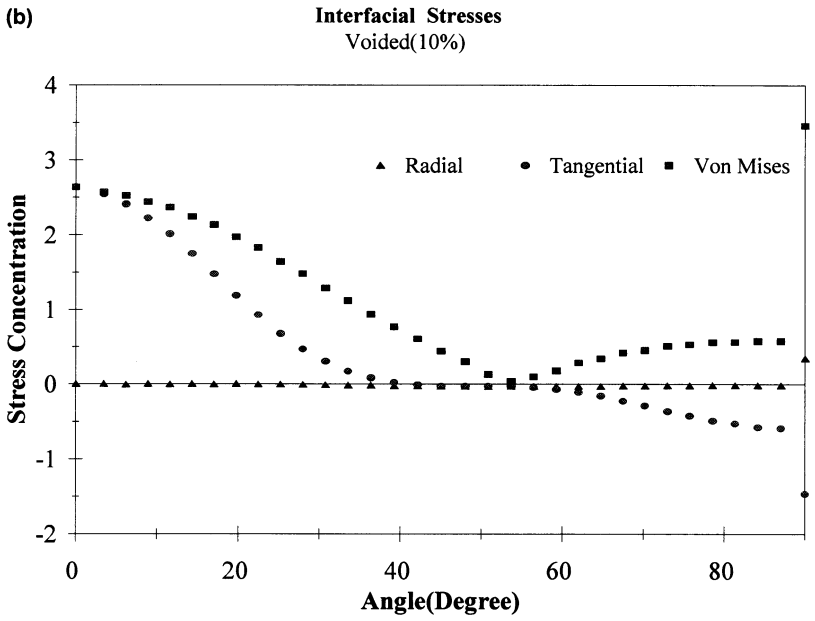

FIGURE 6b Stress concentrations at the border of a void for a porous composite (volume fraction 10%).

These stresses for the composite with fully unbonded filler for different slip coefficients are compared with that obtained for the partly debonded filler particles (Figure 7a–b). Two different volume fractions of 5% and 20% are studied. Only the contacting segments of the interface are considered.

For lower volume fraction (5%) the radial compressive stress reduces for the slipping interface (Figure 7a). The lower the slip coefficient, the lower the friction and the compressive stresses will be. However, the radial stresses at the vicinity of the crack tip show the opposite trend. These stresses are higher for the partly bonded (no slip) case compared with the fully debonded filler (with slip).

At the higher volume fraction of 20%, the stresses at the contacting segment of the interface are very similar in all the cases (Figure 7b). These stresses are very close to zero. However, at the crack tip region, a trend similar to a volume fraction 5% can be observed. The stresses close to the crack tip are higher for the partly bonded (no slip) case compared with the fully de-bonded filler (with slip).

The Von Mises stress and direct stress distribution of a composite with fully debonded particles shows that the maximum stresses are

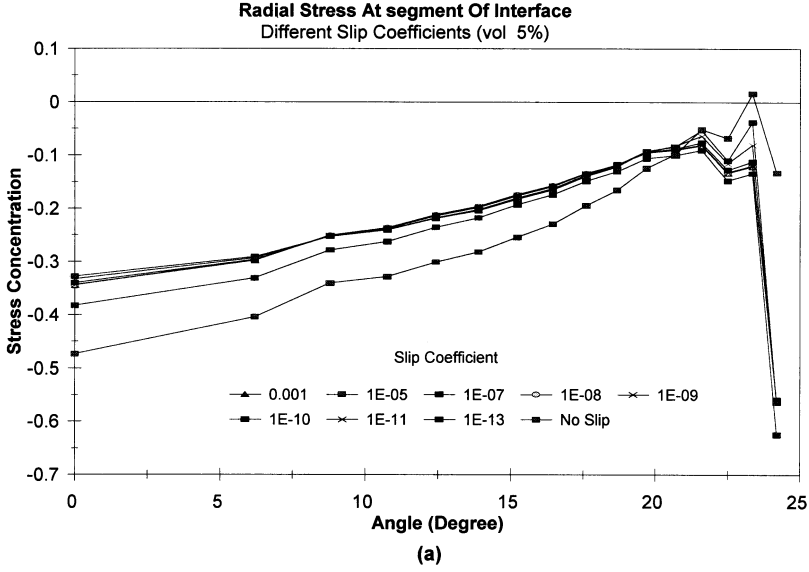

FIGURE 7a Radial stress at the interface of the partly and fully debonded particle with different slip coefficients at the closed segment of the interface (volume fraction = 5%).

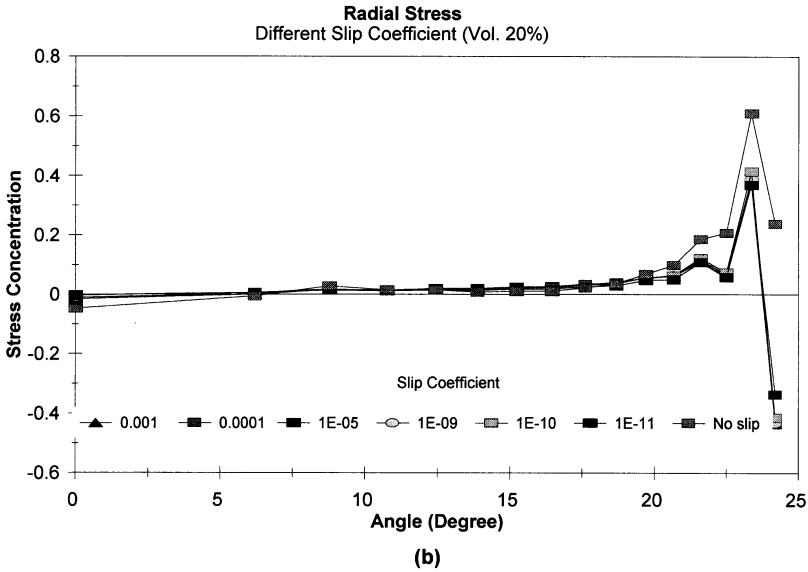

FIGURE 7b Radial stress at the interface of the partly and fully debonded particle with different slip coefficients at the closed segment of the interface (volume fraction = 20%).

observed at the point that the components of the composite start to separate (Figure 8a). In a composite with partially unbonded filler particles caused by an interfacial crack, the maximum stresses are found at the crack tip (Figure 8b). The crack tip is at about the same point as the separation location of matrix and filler for a fully unbonded particle, although the stress patterns are much smoother in the fully debonded case. In a composite containing voids the maximum stresses occur at the void boundary (Figure 8c). The presence of rigid particles, even with fully unbonded surfaces, changes the stress distribution in the matrix compared with a porous composite. This suggests that many of the previous studies that have made the assumption of similar stress states for these two cases need to be revised. For a perfectly bonded composite this maximum is found at the pole of the filler particle (Figure 8d). This makes these materials more ductile.

Stiffness of a Composite with Unbonded Filler

In order to study the effect of the level of the bonding on the stiffness of the composite, the estimated modulus of composites

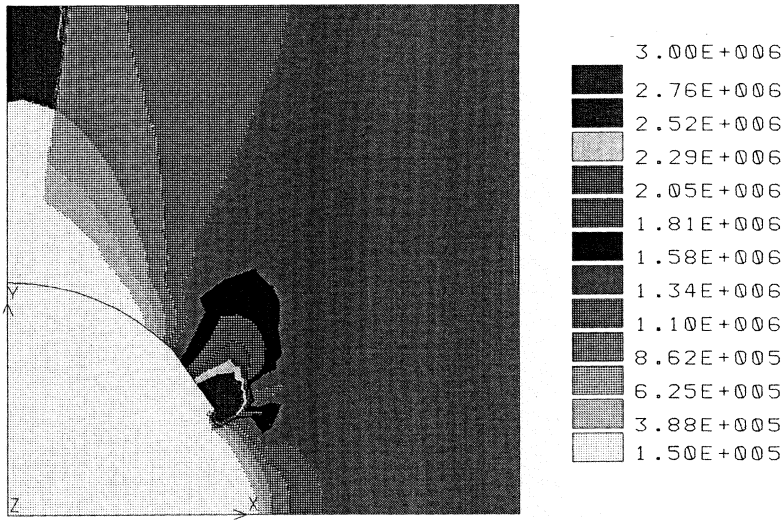

(a) Fully Unbonded Filler

FIGURE 8a Contour diagram of the direct stress concentrations in the composite with fully unbonded filler.

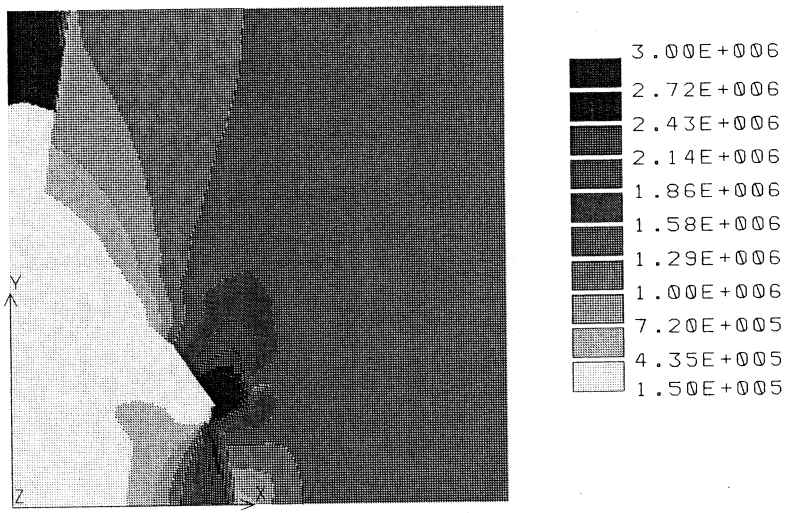

(b) Partly Debonded Filler

FIGURE 8b Contour diagram of the direct stress concentrations in the composite with partially bonded filler.

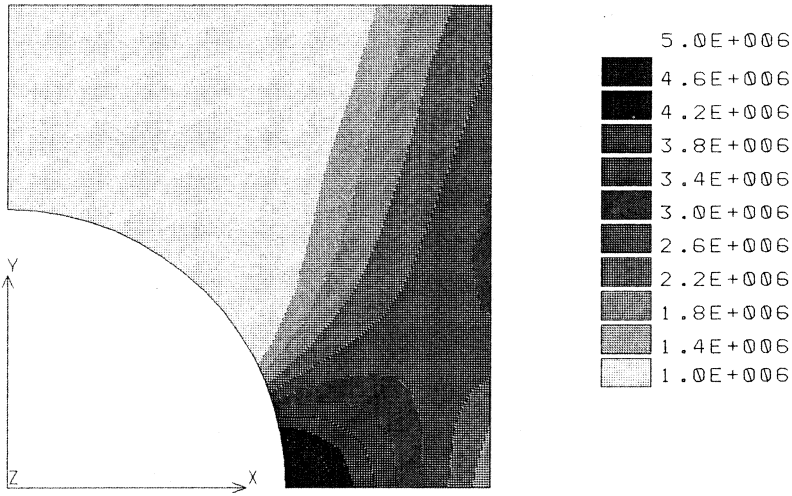

(c) Porous Composite

FIGURE 8c Contour diagram of the direct stress concentrations in a porous composite.

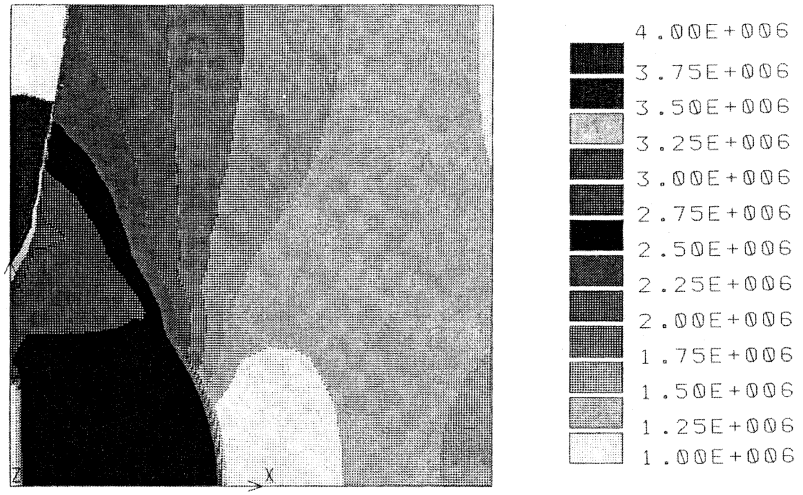

(d) Perfectly Bonded Filler

FIGURE 8d Contour diagram of the direct stress concentrations in the composite with perfectly bonded filler.

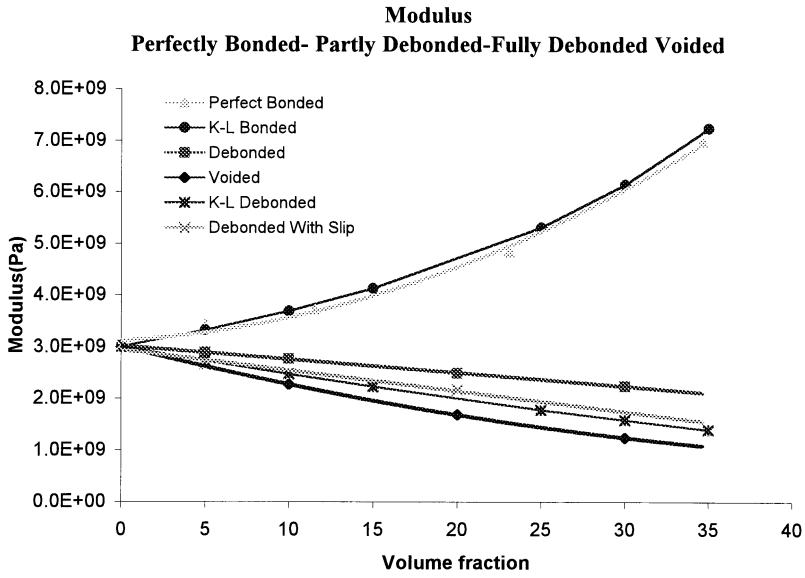

FIGURE 9 Comparison of stiffness of the perfectly bonded, fully and partly debonded particulate and voided composites.

filled with the partially or fully debonded particles and composites containing voids are compared with composites with perfectly bonded particles (Figure 9). Whilst in the perfectly bonded composite the filler volume fraction increases the stiffness, the trend is the opposite for the partially bonded or fully debonded particulate composites.

The fully debonded composite is not efficient in transferring the load from the matrix to filler. Therefore, it shows lower stiffness compared with a partially bonded composite that, at least at the bonded region, transfers the load.

Modulus of composite is a bulk property which depends primarily on the geometry, modulus, particle size distribution, and concentration of the filler and has been represented by a large number of theoretically derived equations. Often one theory gives a better account of one situation than another. One of the better known and widely used models is the Kerner-Lewis Equation [10]:

$$E_c = E_m \frac{1 + A_1 B_1 \phi}{1 - B_1 \psi \phi} \tag{10a}$$

The constant A_1 is determined by the matrix Poisson's ratio as follows:

$$A_1 = \frac{7 - 5v}{8 - 10v} \tag{10b}$$

The other constant, B_1, accounts for the relative modulus of the filler and of the matrix:

$$B_1 = \frac{E_f/E_m - 1}{E_f/E_m + A_1} \tag{10c}$$

with E_f and E_m representing the filler and the matrix moduli, respectively.

The parameter ψ is a crowding factor described as:

$$\psi = 1 + \phi\left(\frac{1 - \phi_m}{\phi_m^2}\right) \tag{10d}$$

φ_m corresponding to the maximum filler volume packing fraction. Equation (10a) is used to evaluate the modulus of a composite containing perfectly bonded and homogeneous filler particles. The result of the Kerner-Lewis estimates for the composite modulus is compared with our finite element model results. The agreement is perfect.

The Kerner-Lewis model for a composite with fully debonded particles is considered similar to the composite with voids. The equation for estimation of modulus of the composite then is modified as:

$$E_c = E_m \frac{1 - \phi}{1 - B_2 \varphi \phi} \tag{11}$$

where $(B_2) = -1/A_1$. The modulus values for a fully debonded composite estimated by the Equation (11) is compared with our finite element model results in Figure 9. The Kerner-Lewis curve lies between the curves of fully debonded and voided composites estimated by our finite element model.

Strength of a Composite with Unbonded Filler

The tensile strength of the composites with perfectly bonded and unbonded interfaces and composites with voids are calculated using the finite element model. In order to calculate the composite strength, it was assumed that the composite would fail as soon as an element of the matrix reached a large enough value of stress to cause fracture of the matrix. Since the matrix is subjected to combined stresses

(triaxial) a suitable failure criterion has to be used in order to predict matrix failure under combined stresses. The Von Mises failure criterion or distortion energy theory was selected.

This criterion is then applied by determining which element has the maximum value of distortion energy for the applied stress. This value of energy may not exceed the value needed to fail the matrix material (σ_{ys}^2) and, thus, the composite strength is calculated from

$$S_c = \sigma_z \frac{\sigma_{ys}}{(U_{\max})^{1/2}} \tag{12}$$

where $U_{\max}$ is the maximum value of distortion energy determined for the arbitrary specified displacement which produces the average stress, σ_z, and S_c is the composite strength. The accuracy of the strength results is particularly affected by the assumption that composite failure occurs upon the first matrix failure. The finite element analysis predicts normally lower strength in comparison with the experimental results.

The results are compared in Figure 10a. The decrease of the tensile strength with increasing volume fraction can be observed in all cases. The graph shows the strength of composite with unbonded interface is between the upper bound curve which is for the bonded interface and the lower bound curve which represents the composites with voids.

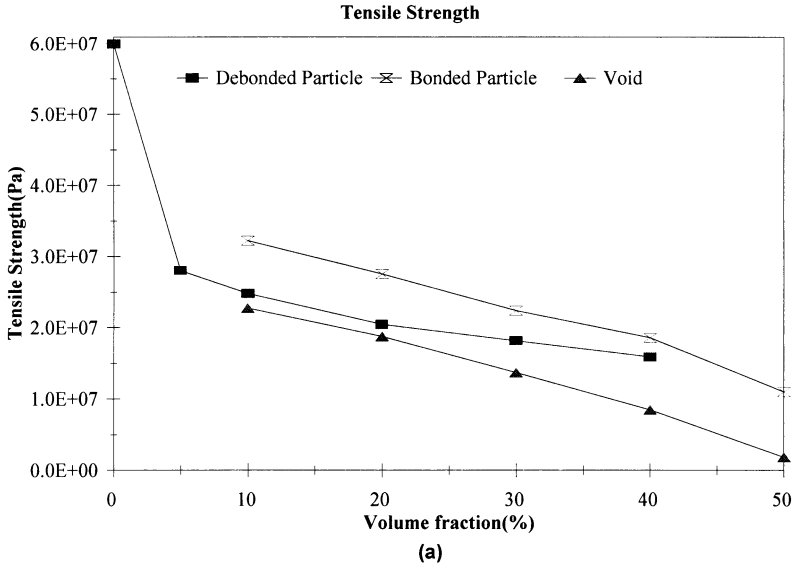

FIGURE 10a Strength of the perfectly bonded, fully debonded and voided composites.

Different theoretical models are suggested for the unbonded or no adhesion case. A commonly reported model is due to Nicolais and Narkis [11] which is based on the assumption that the unbonded particle cannot carry any of the load and the yielding occurs in the minimum cross section of the continuous phase. They presented the following equation for the yield stress of the composite.

$$\sigma_c = \sigma_m(1 - 1.21V_f^{2/3}) \tag{13}$$

Another model suggested by Neilsen [12] gives the yield stress in a composite assuming no adhesion between polymer and filler, expressed as:

$$\sigma_c = \sigma_m(1 - V_f^{2/3})S \tag{14}$$

where S is the stress concentration function which can be determined by the finite element analysis.

In Figure 10b the strength predicted by the finite element analysis is compared with the models proposed by Neilsen and Nicloais and Narkis.

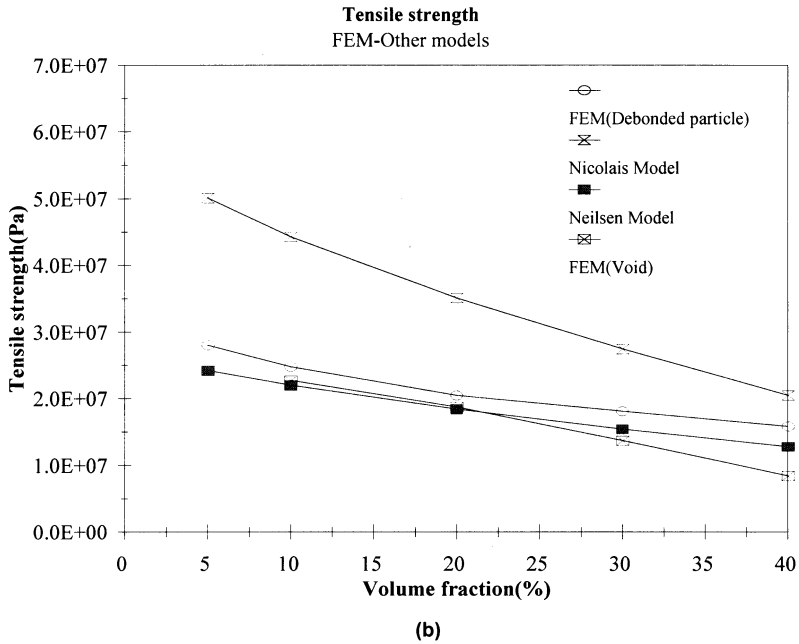

FIGURE 10b Strength of debonded composite predicted by FEM and other models.

Neilsen's prediction is very close to the finite element prediction for voided composites and it is also closer to the unbonded composite. But the Nicolais' and Narkis's model gives a much higher value for the strength.

CONCLUSIONS

A finite element model is developed to predict the stiffness, strength and stress-strain behaviour of filled composites with unbonded particles. The effect of poor adhesion on stress transfer is evaluated and compared with perfectly bonded particulate composites. The computational results are used to predict the further failure progression in particulate composites. The loci of concentration of stress of debonded composites are recognised.

The friction between matrix and filler at the contact points is simulated by imposing the slip condition. The slip coefficient indicates the level of friction between the components of the composite. In most of the previous models the case of fully unbonded particles is considered similar to a composite containing voids. The stress at the interface is considered to be similar to that of a porous composite. Our analysis clearly shows that, even in the case of fully unbonded filler, a part of the interface of matrix and filler stay in contact. The load is transferred at this segment. This changes the distribution of the stresses at the interface compared with a void. Whereas a porous composite is tougher because of the lack of concentration of stresses, it is much weaker than a composite with fully unbonded rigid particles.

In a composite with unbonded filler, the initial slipping contact surfaces might become separated. This separation starts from the equator. This leads to a state of slip-stick at the interface with unstable stresses. In a composite with an interfacial crack the propagation is stable.

REFERENCES

[1] Moloney, A. C. and H. H. Kausch, *J. Mater. Sci*. **22**(2), 381 (1987).
[2] Sato, Y. and J. Furukawa, *Rubber Chem. Technol*. **36**, 1081 (1963).
[3] Brassell, G. W. and K. B. Wischmann, *J. Mater. Sci.* **9**, 307 (1974).
[4] Ahmed, S. and F. R. Jones, *J. Mater. Sci.* **25**, 4933 (1990).
[5] Ghassemieh, E. and V. Nassehi, *Advances in Polymer Technology*, **1**, 42 (2001).
[6] Zienkiewics, O. C. and R. L. Taylor, *The finite element method*, Vol. 1 (McGraw-Hill, New York, 1988).
[7] Agrawal, B. D. and L. J. Broutman, *Fibre Sci. and Tech.*, **7**, 63 (1974).
[8] Ghassemieh, E., J. Petera and V. Nassehi, ICHEME Research Event, 329 (1996).
[9] Ghassemieh, E., to be published in *Composite Science and Technology.*
[10] Skovby, M. H. B., R. Lessel, and J. Kops, *J. Polym. Sci. Polym. Chem.*, **28**, 75 (1990).
[11] Nicolais, L. and M. Narkis, *Polym. Eng. Sci*., **11**, 194 (1971).
[12] Neilsen, L. E., *J. Appl. Polym. Sci*., **10**, 97 (1966).

APPENDIX:

Deriving the Working Equations

We start with the governing equations of creeping (Stokes) flow of incompressible fluids. Using an axisymmetric *r-z* coordinate system the momentum equations describing such regimes are given as:

$$-\frac{\partial P}{\partial z}+\mu\left[\frac{1}{r}\frac{\partial}{\partial r}\left(r\frac{\partial v_r}{\partial r}\right)+\frac{\partial^2 v_z}{\partial z^2}\right]+\rho g_z=0 \tag{1A}$$

$$-\frac{\partial P}{\partial r}+\mu\left[\frac{\partial}{\partial r}\left(\frac{1}{r}\frac{\partial}{\partial r}(rv_r)\right)+\frac{\partial^2 v_r}{\partial z^2}\right]+\rho g_r=0 \tag{2A}$$

The continuity equation is given as:

$$\frac{\partial v_r}{\partial r}+\frac{v_r}{r}+\frac{\partial v_z}{\partial z}=0 \tag{3A}$$

where v_r, v_z are velocity components, P is the pressure, μ represents fluid viscosity, ρ is fluid density and g_r, g_z are the components of the body force vector.

In the continuous penalty method, the incompressibility condition described by Equation (3A) is treated as a constraint on the momentum Equations (1A) and (2A). In this approach, the pressure in the momentum equation is eliminated as an unknown field variable through the use of a penalty parameter as follows:

$$P=-\lambda\left(\frac{\partial v_r}{\partial r}+\frac{v_r}{r}+\frac{\partial v_z}{\partial z}\right) \tag{4A}$$

where λ is a penalty parameter (usually a very large number). The penalty parameter in our case is defined as:

$$\lambda=2\nu\mu/(1-2\nu) \tag{5A}$$

where ν is the Poisson ratio. Substitution of the pressure in the Stokes flow equations using Equation (4A) results in a set of equations which are identical to the equations of equilibrium of elastic solids given as:

$$-\frac{\partial}{\partial r}\left(\frac{\partial v_r}{\partial r}+\frac{v_r}{r}+\frac{\partial v_z}{\partial z}\right)+\frac{\partial}{\partial r}\left(2\mu\frac{\partial v_r}{\partial r}\right)+\frac{2\mu}{r}\frac{\partial v_r}{\partial r}-\frac{2\mu v_r}{\partial r^2}$$

$$+\frac{\partial}{\partial z}\left[\mu\left(\frac{\partial v_r}{\partial z}+\frac{\partial v_z}{\partial r}\right)\right]=0 \tag{6A}$$

$$-\frac{\partial}{rz}\left(\frac{\partial v_r}{\partial r}+\frac{v_r}{r}+\frac{\partial v_z}{\partial z}\right)+\frac{\partial}{rz}\left(2\mu\frac{\partial v_r}{\partial r}\right)+\frac{\mu}{r}\left(\frac{\partial v_z}{\partial r}+\frac{\partial v_r}{\partial z}\right)$$

$$+\frac{\partial}{\partial z}\left[\mu\left(\frac{\partial v_r}{\partial z}+\frac{\partial v_z}{\partial r}\right)\right]=0 \tag{7A}$$

The Galerkin weighted residual method is used to derive the weak formulation of Equations (6A) and (7A). After the application of Green's theorem to reduce the order of the differentiation of the second order terms in these equations, the weak forms in the r and z directions are obtained as:

$$\int_\Omega\left[\lambda\left(\frac{N_jN_i}{r^2}+\frac{N_j}{r}\frac{\partial N_i}{\partial r}+\frac{N_i}{r}\frac{\partial N_j}{\partial r}+\frac{\partial N_j}{\partial r}\frac{\partial N_i}{\partial r}\right)\right.$$

$$\left.+\mu\left(\frac{2N_jN_i}{r^2}+\frac{N_j}{\partial r}\frac{\partial N_i}{\partial r}+\frac{\partial N_j}{\partial z}\frac{\partial N_i}{\partial z}\right)\right]U_i r dr dz$$

$$+\int_\Omega\lambda\left[\left(\frac{\partial N_j}{\partial r}\frac{\partial N_i}{\partial z}+\frac{1}{r}N_j\frac{\partial N_i}{\partial z}\right)+\mu\left(\frac{\partial N_j}{\partial z}\frac{\partial N_i}{\partial r}\right)\right]V_i r dr dz$$

$$+\oint_\Gamma\left(\mu N_i\frac{\partial N_j}{\partial z}rn_z+2\mu N_i\frac{\partial N_j}{\partial r}rn_r-\lambda N_i\frac{\partial N_j}{\partial r}rn_r-\lambda N_iN_jn_r\right)U_i d\Gamma$$

$$+\oint_\Gamma\left(\mu N_i\frac{\partial N_j}{\partial r}rn_z-\lambda N_i\frac{\partial N_j}{\partial z}n_r\right)V_i d\mathrm{T}=0\quad(r\text{ component}) \tag{8A}$$

$$\int_\Omega\lambda\left[\left(\frac{\partial N_j}{\partial z}\frac{\partial N_i}{\partial r}+\frac{1}{r}N_i\frac{\partial N_j}{\partial z}\right)+\mu\left(\frac{\partial N_j}{\partial r}\frac{\partial N_i}{\partial z}\right)\right]V_i r dr dz$$

$$+\int_\Omega\lambda\left[\left(\frac{\partial N_j}{\partial z}\frac{\partial N_i}{\partial z}\right)+\mu\left(2\frac{\partial N_j}{\partial z}\frac{\partial N_i}{\partial r}\right)\right]V_i r dr dz$$

$$+\oint_\Gamma\left(\mu N_i\frac{\partial N_j}{\partial z}rn_r-\lambda N_i\frac{\partial N_j}{\partial r}rn_z-\lambda N_iN_jn_z\right)U_i d\Gamma$$

$$+\oint_\Gamma\left(2\mu N_i\frac{\partial N_j}{\partial z}rn_z+\mu N_i\frac{\partial N_j}{\partial r}rn_r-\lambda N_i\frac{\partial N_j}{\partial z}rn_z\right)V_i d\Gamma=0$$

$$(z\text{ component}) \tag{9A}$$

In the above equations μ is shear modulus, λ is penalty parameter, n_z, n_r are components of unit vector normal to the boundary in the outward direction, N_i and N_j are the weight and shape functions, respectively.

Equations (8A) and (9A) are the working equations of the present scheme. In this study we have based our model on the Stokes flow equations and the penalty method which is identical to the commonly used equilibrium finite element approach for elasticity analysis. This gives us the flexibility to switch the model from the analysis of fluid flow to solid material deformation under applied loads. Since most composite materials are in a fluid state at the processing time and are in a solid state when they are used, this approach offers the advantage of the ability to predict the material behaviour in both cases using the same computer model.